Fusion hindrance for the positive Q-value system ^{12}C+^{30}Si

F. Galtarossa[1,⋆], *A. M.* Stefanini[1,⋆⋆], *G.* Montagnoli[2], *C. L.* Jiang[3], *G.* Colucci[2], *S.* Bottoni[3], *C.* Broggini[2], *A.* Caciolli[2], *P.* Colović[4], *L.* Corradi[1], *S.* Courtin[5], *R.* Depalo[2], *E.* Fioretto[1], *G.* Fruet[5], *A.* Gal[5], *A.* Goasduff[1], *M.* Heine[5], *S. P.* Hu[6], *M.* Kaur[7], *T.* Mijatović[4], *D.* Montanari[5], *F.* Scarlassara[2], *E.* Strano[2], *S.* Szilner[4], and *G. X.* Zhang[8]

[1] *INFN, Laboratori Nazionali di Legnaro, I-35020 Legnaro (PD), Italy*
[2] *Dip. di Fisica e Astronomia, Univ. di Padova, and INFN-PD, I-35131 PD, Italy*
[3] *Physics Division, Argonne National Laboratory, Argonne, IL 60439, USA*
[4] *Ruđer Bošković Institute Zagreb, Croatia*
[5] *IPHC, CNRS-IN2P3, Université de Strasbourg, F-67037 Strasbourg Cedex 2, France*
[6] *College of Phys. Sci. and Tech., Shenzhen Univ., Shenzeng, 518060, China*
[7] *Department of Physics, Punjab Technical University Jalandhar, Kapurthala, India*
[8] *School of Phys. and Nucl. Energy Eng., Beihang Univ., Beijing, 100191, China*

Abstract. The fusion excitation function for the positive-Q-value system ^{12}C+^{30}Si (Q_{fus} = +14.1 MeV) has been measured in inverse kinematics down to the μb level and compared with standard coupled-channel calculations. The appearance of the fusion hindrance phenomenon and the evidence of a S-factor maximum have been observed. This result can be significant to extrapolate the behavior of lighter astrophysical relevant systems at deep sub-barrier energies, where existing experimental data are still contradicting and affected by large errors.

1 Introduction

Fusion reactions between light heavy ions have a prominent role in the dynamical stellar evolution. Reactions such as ^{12}C+^{12}C, ^{12}C+^{16}O and ^{16}O+^{16}O are the main processes during the carbon and oxygen burning stages of massive stars [1, 2]. Existing data for these systems do not extend in the energy range of typical astrophysical scenarios because at the involved temperatures (T $\sim 10^9$ K) the associated Gamow energies are well below the Coulomb barrier V_C. For this reason the available data sets are still contradicting and affected by large errors, due to the significant experimental difficulties in measuring cross sections in the subnanobarn range. An example is reported in figure 1 where the S factors (see Sect. 2) for fusion between ^{12}C and ^{12,13}C are plotted as a function of E/V_C. No clear conclusion about the reaction rates in stars can be safely drawn from these data.

In order to obtain the astrophysical reaction rates one has, therefore, to rely on phenomenological extrapolation methods [3]. In particular, the possible presence of fusion hindrance and the trend of the S factor at very low energies for medium-light systems may assume a relevant role in the extrapolation procedure. If the S factor develops a maximum, the fusion cross sections and consequently the reaction rates in stars at the lower energies important for astrophysics will be substantially lower than what predicted by simple extrapolations of the high-energy trends, where sets of measurements already exist.

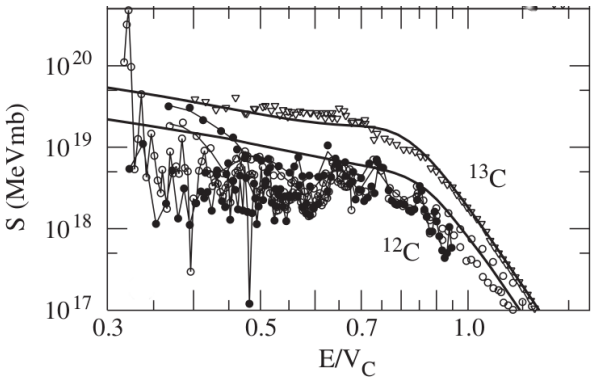

Figure 1. Measured S factors of fusion between ^{12}C and ^{12,13}C as a function of E/V_C. The two solid lines are theoretical predictions from coupled-channels calculations. Taken from Ref. [1].

In this contribution we will present the preliminary results of a measurement performed at the Laboratori Nazionali of Legnaro of INFN where the excitation function for the system ^{12}C+^{30}Si was measured down to the deep sub-barrier energy regime. The measurement was done by separating the evaporation residues from the beam by means of an electrostatic deflector and then detecting them in the E-ΔE-ToF spectrometer widely used in recent years for similar experiments. The aim of the experiment was to look for an indication of fusion hindrance in this positive Q-value system and the possible presence of a S-

⋆ e-mail: franco.galtarossa@lnl.infn.it
⋆⋆ e-mail: alberto.stefanini@lnl.infn.it

factor maximum, which would be a relevant clue to deduce the behavior of astrophysical relevant systems.

2 Fusion hindrance and S factor

Since its discovery about 15 years ago [4], the phenomenon of fusion hindrance at low energies has been observed in many medium-heavy systems [1]. Its signature is a steeper decrease of the fusion cross section in the deep sub-barrier regime with respect to coupled-channels (CC) calculations employing a standard Woods-Saxon (WS) potential. Experimental data can be reproduced by using different potentials, as for instance the M3Y with the addition of a repulsive term [5, 6].

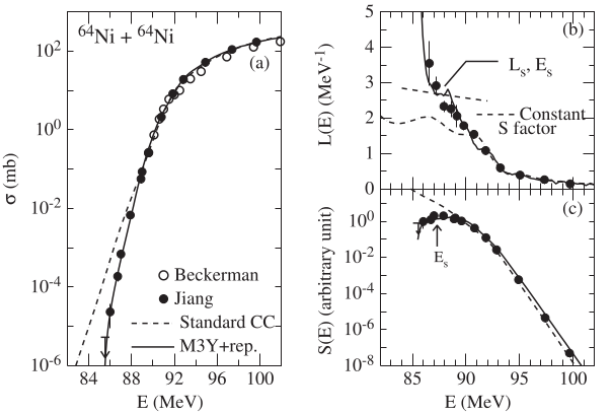

Figure 2. Experimental fusion cross section (a), logarithmic derivative (b) and S factor (c) for the system ^{64}Ni+^{64}Ni. Solid circles are from Ref. [7], open circles from Ref. [8]. The dash and solid curves represent calculations with a standard Woods-Saxon potential and with the M3Y+rep. potential, respectively. Taken from Ref. [1].

An alternative way to make evident the presence of hindrance, without invoking model calculations, is to introduce the logarithmic derivative of the energy-weighted cross section, L(E), and the S factor, S(E), which are defined as:

$$L(E) = \frac{d[ln(E\sigma)]}{dE} = \frac{1}{E\sigma}\frac{d(E\sigma)}{dE} \quad (1)$$

$$S(E) = E\sigma(E)e^{2\pi\eta} \quad (2)$$

where $\eta = Z_1Z_2e^2/\hbar v$ is the Sommerfeld parameter. The onset of hindrance can usually be visualized with S(E) reaching a maximum and L(E) crossing the logarithmic derivative for a costant S factor, $L_{CS}(E) = \pi\eta/E$, obtained by imposing the maximum condition for S(E). This is shown in figure 2 for the benchmark case ^{64}Ni+^{64}Ni [7]. There is no fundamental principle underlying the constant S factor nor the intersection between L(E) and $L_{CS}(E)$ but they represent a simple and direct way to observe the discrepancy between data and standard CC calculations. The energy E_s at which the maximum appears is usually taken as the threshold energy for hindrance.

Medium-heavy systems, namely those with $\zeta = Z_1Z_2\sqrt{\frac{A_1A_2}{A_1+A_2}} > 1500$, are usually associated with negative ground-state Q values for fusion, $Q_{fus} < 0$. For these systems the S factor always shows a maximum, due to energy conservation considerations: when the center-of-mass energy E_{cm} tends to $-Q_{fus}$, the fusion cross section, and then S, must tend to 0. Figure 3 shows the experimental S factors as a function of the center-of-mass energy for different negative Q-value systems (except for ^{40}Ca+^{48}Ca) where the fusion hindrance was observed. They all develop a maximum.

The same is not true for systems with $Q_{fus} > 0$: when E_{cm} tends to 0, the fusion cross section does not necessarily tend to 0 and neither does S. Of course the extrapolation of the behavior of these systems to lower energies largely depends on whether or not the S factor develops a maximum.

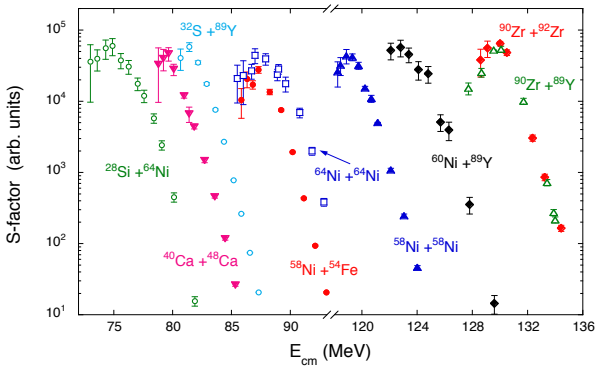

Figure 3. Experimental S factors as a function of the center-of-mass energy for different negative-Q-value systems (except for ^{40}Ca+^{48}Ca which has Q_{fus} = +4.56 MeV).

Recent experiments investigated the presence of hindrance in systems with positive Q_{fus}. Fusion excitation functions were measured for the systems ^{28}Si+^{30}Si (Q_{fus} = +14.3 MeV) [9, 10], ^{36}S+^{48}Ca (Q_{fus} = +7.55 MeV) [11] and ^{27}Al+^{45}Sc (Q_{fus} = +9.63 MeV) [12] down to ~ 4 μb, 600 nb and 300 nb, respectively. By comparing data with standard CC calculations, in all the systems indications of fusion hindrance were observed. On the other hand, no clear S-factor maxima showed up in the energy ranges covered by the experiments.

More recently indications of S-factor maxima were observed in the system ^{40}Ca+^{48}Ca (Q_{fus} = +4.56 MeV) [13] and more clearly in ^{24}Mg+^{30}Si (Q_{fus} = +17.9 MeV) [14]. This observation suggests that the cross section falls off very steeply at even lower energies than the measured ones and this behavior might be common to other positive Q-value systems, such as those involved in the carbon burning of stars.

In this context the ^{12}C+^{30}Si system (Q_{fus} = +14.1 MeV), which is not itself a relevant case in astrophysics, may represent a critical case to predict the behavior of lighter systems like ^{12}C+^{12}C, ^{12}C+^{16}O and ^{16}O+^{16}O. Figure 4 (top) shows the systematics for several medium-light

systems with $Q_{fus} > 0$ (in red) and $Q_{fus} < 0$ (in black) where E_s is plotted as a function of the parameter ζ previously defined (μ is the reduced mass of the system). The points for $^{12}C+^{12}C$ and $^{16}O+^{16}O$ are not directly measured and rely on extrapolations. Figure 5 shows the similar systematics for the measured (red) and extrapolated (black) threshold cross section, σ_s, for some medium-light systems. One can clearly see that the measurement of E_s and σ_s for $^{12}C+^{30}Si$, whose position in ζ is indicated by the blue arrows in the figures, could be relevant for a more reliable extrapolation.

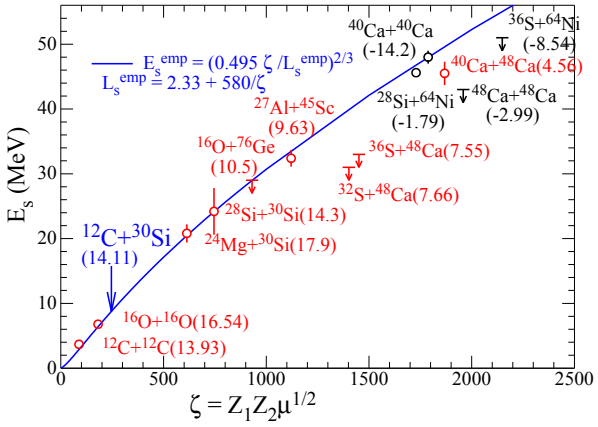

Figure 4. Systematics of threshold energies for hindrance, E_s, for various medium-light systems with positive (red) and negative (black) Q values for fusion. The points for $^{12}C+^{12}C$ and $^{16}O+^{16}O$ are determined from extrapolation procedures. The blue line is the predicted threshold for hindrance on the basis of the phenomenological systematics of Jiang et al. [18]. The predicted location for $^{12}C+^{30}Si$ is indicated by the blue arrow.

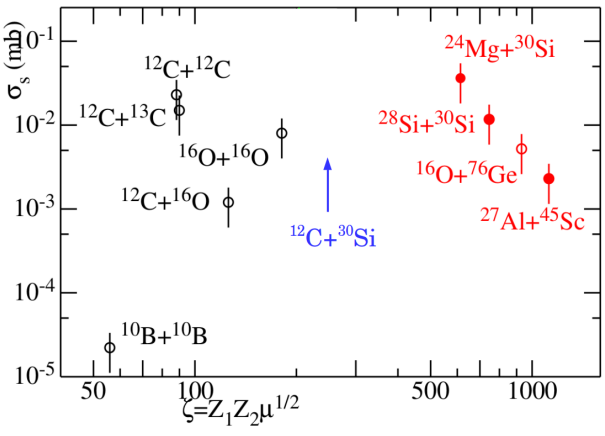

Figure 5. Systematics of threshold cross sections for hindrance, σ_s, for various medium-light systems determined by measurements (red) or by extrapolations (black). The predicted location for $^{12}C+^{30}Si$ is indicated by the blue arrow.

Existing data for this system [15], and for the nearby $^{12}C+^{28}Si$ [16, 17], extended down to ~ 200 mb, too far from the range in which the hindrance could start to play a role. Moreover, these data exhibit large error bars. The aim of our experiment was to refine and extend the measurement of the excitation function down in energy as much as possible to search for a possible indication of hindrance.

3 Experiment

The experiment was performed at the Laboratori Nazionali of Legnaro of INFN (Padova, Italy). The ^{30}Si beam was provided by the XTU Tandem accelerator in the energy range ~ 33-80 MeV, with an intensity of ~ 10 pnA. The 50 μg/cm^2 ^{12}C targets, enriched to 99.9% in mass 12 to reduce as much as possible the contamination coming from the higher-mass ^{13}C isotope, were installed in a sliding-seal scattering chamber. The choice of the inverse kinematics allowed to produce the compound nucleus (CN) with enough kinetic energy to reach the detector telescope, and still produce a signal in the Si detector of sufficient amplitude to start the Time-of-Flights (ToF) and trigger the DAQ. On the other hand, since the electric rigidities of CN and scattered beam are more similar compared to direct kinematics conditions, the contribution of background components might be more significant in this case.

The evaporation residues (ER), separated from the beam in the electrostatic deflector [20], were detected at $\theta_{lab} = 3°$ with a E-ΔE-ToF telescope schematically depicted in figure 6 and described in more detail in Ref. [19].

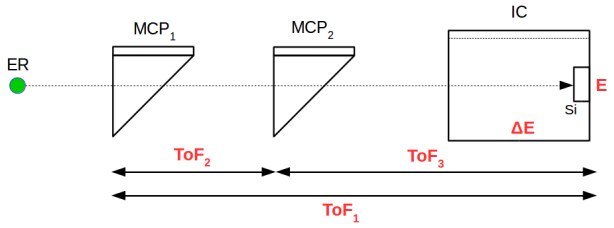

Figure 6. The E-ΔE-ToF telescope following the electrostatic deflector. Measured quantities are labeled in red.

The measured quantities are three ToFs, an energy loss ΔE in the ionisation chamber (IC) and a residual energy E in the silicon detector (Si). Four silicon detectors, placed around the target at $\theta_{lab} = 16°$ with respect to the beam direction, in the up, down, right and left position, were used for beam control and normalization between the different runs by measuring the Rutherford scattering from the target. Three angular distributions were measured at $E_{lab} = 45$, 59 and 80 MeV in the range $-6° \leq \theta_{lab} \leq +10°$. We report in figure 7 the angular distribution obtained at $E_{lab} = 59$ MeV (points), together with the gaussian curve which well fits the data.

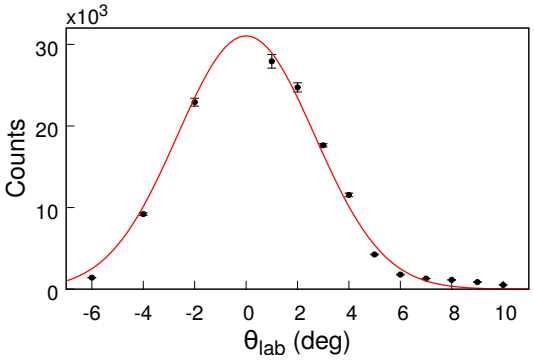

Figure 7. Angular distribution of the ER at E_{lab} = 59 MeV (points). The curve represents a gaussian fit. The plotted errors are only statistical uncertainties.

The evaporation residues can be separated from the scattered beam in the online analysis by combining E-ToF and E-ΔE matrices. Figure 8 shows an example of two-dimensional spectra where the residual energy detected in the Si detector is plotted versus the ToF between the first MCP detector and the Si detector at two different bombarding energies, one above (top panel) and the other below (bottom panel) the barrier. The ER are in both cases well separated from the beam.

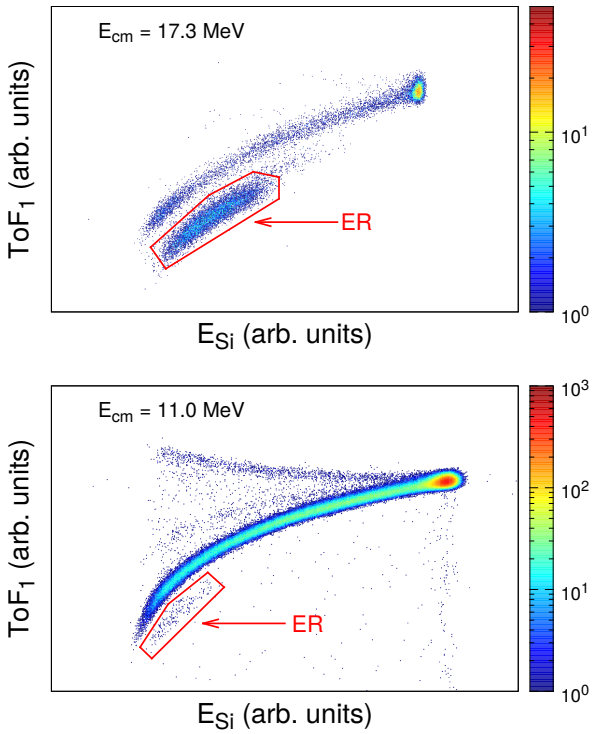

Figure 8. Two-dimensional spectra ToF-E for the present experiment at the indicated bombarding energies, above (top) and below (bottom) the Coulomb barrier. Evaporation residues are in both cases well separated from the scattered beam.

4 Results

Figure 9 shows the resulting excitation function. To account for a possible contamination from higher-mass carbon isotopes, some points were measured with a ^{13}C target and used to correct the plotted cross sections. The energy loss in the target was taken into account as well in the analysis. The new data well agree with those of Ref. [15] but extend down to a cross section almost 5 orders of magnitude lower.

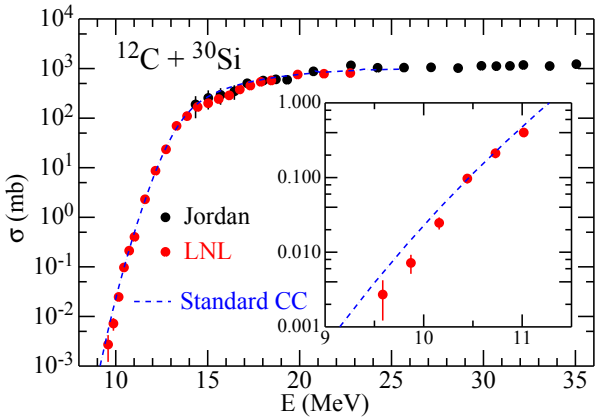

Figure 9. Experimental excitation functions measured in Ref. [15] (black points) and in the present experiment (red points), together with standard CC calculations (dashed blue line). In the insert a zoom in the low-energy region is shown.

Experimental data were compared to preliminary CC calculations employing an Akyüz-Winther (AW) potential [21]. Since the 2^+ and 3^- states of ^{12}C are quite high in energy (4.44 and 9.64 MeV, respectively), in the calculations this nucleus was considered inert. It is well known that the effect of coupling to high-lying states in CC calculations mainly consists in an overall shift of the calculated cross section to slightly lower energies, without significant influence on the shape of the excitation function [22, 23]. This coupling can then be accounted for by an adiabatic renormalization of the ion-ion potential in order to reproduce the experimental cross sections in the vicinity of the barrier. For this reason the depth of the AW potential here used was slightly modified and its value set to V_0 = 48.24 MeV. The parameter r_0, which accounts for the radii of the interacting nuclei, and the diffuseness a were set to 1.10 fm and 0.61 fm, respectively. This potential produces a barrier V_c = 13.6 MeV.

For the ^{30}Si the CC calculations included the coupling to the 2^+ and 3^- states, whose energies E and deformation parameters β_λ are reported in table 1. We remind that the deformation parameter is related to the reduced transition probability of the electromagnetic decay from the excited state λ^π to the ground state by [1]:

$$\beta_\lambda^2 = \left(\frac{4\pi}{3Ze^2R^\lambda}\right)^2 4\pi B(E\lambda) \ , \qquad (3)$$

with Z and R the nuclear charge and radius, respectively.

Table 1. Parameters for the low-lying excited states of ^{30}Si.

λ^{π}	E (MeV)	β_{λ}
2^{+}	2.235	0.33
3^{-}	5.488	0.28

In the insert of figure 9 one can see how the CC calculations start to overpredict the experimental cross sections from E ~ 10.5 MeV, an indication that the fusion hindrance is present in the measured energy range.

To confirm this hypothesis we report in figure 10 the experimental and calculated logarithmic derivative L(E) and the experimental S factor S(E).

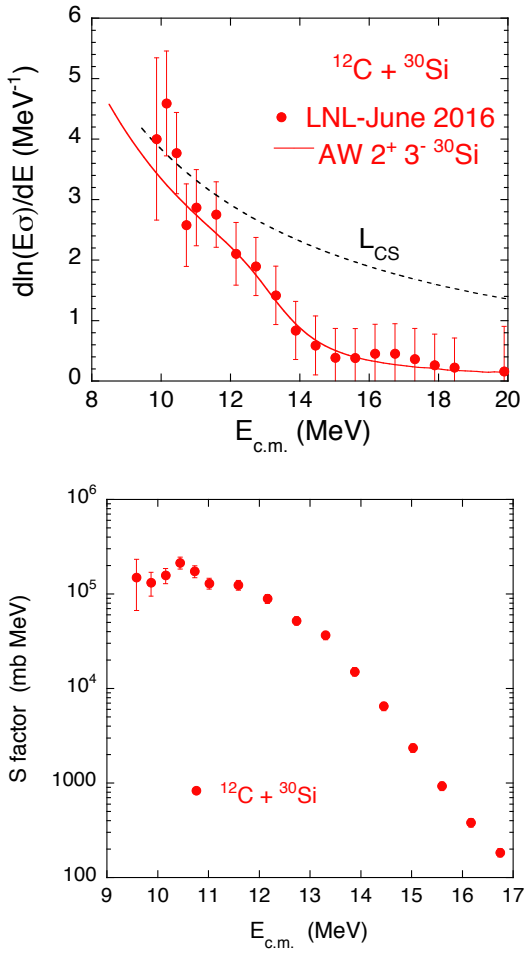

Figure 10. Experimental logarithmic derivative (top) and S factor (bottom) for the present experiment. For L(E) preliminary standard CC calculations are plotted as well.

The plotted values L_i(E) were obtained by calculating the difference quotient:

$$L_i(E) = \frac{[ln(E\sigma)]_{i+1} - [ln(E\sigma)]_i}{E_{i+1} - E_i} \quad . \tag{4}$$

Though the quite large error bars, one can clearly notice a crossing of the $L_{CS}(E)$ function, which was introduced in Sect. 2, as well as the appearance of a maximum of the S factor around E = 10.5 MeV. This can be taken as a confirmation of the onset of hindrance for this positive Q-value system.

5 Conclusions

In this contribution we have described the measurement of the fusion excitation function for the positive Q-value system ^{12}C+^{30}Si in inverse kinematics, performed at the INFN Laboratori Nazionali of Legnaro. The aim of the experiment was to search for a possible indication of fusion hindrance and presence of a S-factor maximum in this system, which could positively lead the extrapolation to lower mass systems that are relevant in an astrophysical context. The evaporation residues, separated from the beam by means of an electrostatic deflector, were detected with a E-ΔE-ToF telescope. The excitation function has been extended down to ~ 3 μb, nearly 5 orders of magnitude lower than existing measurements for this system. We could observe the presence of fusion hindrance by comparing the experimental cross sections with preliminary standard CC calculations which took into account the coupling to the 2^{+} and 3^{-} states of ^{30}Si and consider the ^{12}C as inert. The observation of the crossing between the logarithmic derivative L(E) and L_{CS} and the apperance of a maximum of the S factor give a further confirmation of the presence of hindrance in the measured energy range and are relevant for the extrapolation procedure to lower energies.

The analysis is still ongoing. We expect that more accurate calculations, employing for example a "shallow" potential, will allow to determine more reliably the threshold energy and cross section for hindrance, adding an important point in the systematics of figures 4 and 5.

References

[1] B. B. Back, H. Esbensen, C. L. Jiang and K. E. Rehm, Rev. Mod. Phys. **86**, 317 (2014).
[2] C. J. Horowitz, H. Dussan and D. K. Berry, Phys. Rev. C **77**, 045807 (2008).
[3] C. L. Jiang *et al.*, Phys. Rev. C **75**, 015803 (2007).
[4] C. L. Jiang *et al.*, Phys. Rev. Lett. **89**, 052701 (2002).
[5] S. Misicu and H. Esbensen, Phys. Rev. Lett. **96**, 112701 (2006).
[6] H. Esbensen, C. L. Jiang, and A. M. Stefanini, Phys. Rev. C **82**, 054621 (2010).
[7] C. L. Jiang *et al.*, Phys. Rev. Lett. **93**, 012701 (2004).
[8] M. Beckerman *et al.*, Phys. Rev. Lett. **45**, 1472 (1980).
[9] C. L. Jiang *et al.*, Phys. Rev. C **78**, 017601 (2008).
[10] G. Montagnoli *et al.*, Phys. Rev. C **90**, 044608 (2014).
[11] A. M. Stefanini *et al.*, Phys. Rev. C **78**, 044607 (2008).
[12] C. L. Jiang *et al.*, Phys. Rev. C **81**, 024611 (2010).
[13] C. L. Jiang *et al.*, Phys. Rev. C **82**, 041601(R) (2010).
[14] C. L. Jiang *et al.*, Phys. Rev. Lett. **113**, 022701 (2014).
[15] W. J. Jordan, J. V. Maher and J. C. Peng, Phys. Lett. B **87**, 38 (1979).

[16] S. Gary and C. Volant, Phys. Rev. C. **25**, 1877 (1982).
[17] Y. Nagashima *et al.*, Phys. Rev. C. **26**, 2661 (1982).
[18] C. L. Jiang, B. B. Back, R. V. F. Janssens and K. E. Rehm, Phys. Rev. C **75**, 057604 (2007).
[19] A. M. Stefanini *et al.*, Phys. Rev. C **82**, 014614 (2010).
[20] S. Beghini *et al.*, Nucl. Instr. Meth. A **239**, (1985) 585.
[21] Ö. Akyüz and A. Winther, "*Nuclear structure and heavy-ion physics*", Proc. Int. School of Physics Enrico Fermi, Varenna, edited by R. A. Broglia and R. A. Ricci (North Holland, Amsterdam, 1981) (1981): 492.
[22] N. Takigawa, K. Hagino, M. Abe and A. B. Balantekin, Phys. Rev. C **49**, 2630 (1994).
[23] K. Hagino and N. Takigawa, Prog. Theor. Phys. **128**, 1001 (2012).